Phase-locking and coherent power combining of broadband linearly chirped optical waves

Naresh Satyan,[1,*] Arseny Vasilyev,[1] George Rakuljic,[2] Jeffrey O. White,[3] and Amnon Yariv[1]

[1]*Department of Applied Physics and Materials Science, California Institute of Technology, 1200 E. California Blvd. 136-93, Pasadena, CA 91125, USA*
[2]*Telaris Inc., 2118 Wilshire Blvd. #238, Santa Monica, CA 90403, USA*
[3]*Army Research Laboratory, 2800 Powder Mill Road, Adelphi, MD 20783, USA*
[*]*naresh@caltech.edu*

Abstract: We propose, analyze and demonstrate the optoelectronic phase-locking of optical waves whose frequencies are chirped continuously and rapidly with time. The optical waves are derived from a common optoelectronic swept-frequency laser based on a semiconductor laser in a negative feedback loop, with a precisely linear frequency chirp of 400 GHz in 2 ms. In contrast to monochromatic waves, a differential delay between two linearly chirped optical waves results in a mutual frequency difference, and an acoustooptic frequency shifter is therefore used to phase-lock the two waves. We demonstrate and characterize homodyne and heterodyne optical phase-locked loops with rapidly chirped waves, and show the ability to precisely control the phase of the chirped optical waveform using a digital electronic oscillator. A loop bandwidth of ~ 60 kHz, and a residual phase error variance of < 0.01 rad^2 between the chirped waves is obtained. Further, we demonstrate the simultaneous phase-locking of two optical paths to a common master waveform, and the ability to electronically control the resultant two-element optical phased array. The results of this work enable coherent power combining of high-power fiber amplifiers—where a rapidly chirping seed laser reduces stimulated Brillouin scattering—and electronic beam steering of chirped optical waves.

OCIS codes: (140.3298) Laser beam combining; (140.3600) Lasers, tunable; (030.1640) Coherence.

References and links

1. H. Philipp, A. Scholtz, E. Bonek, and W. Leeb, "Costas loop experiments for a 10.6 μm communications receiver," IEEE Trans. Commun. **31**, 1000–1002 (1983).
2. S. Saito, O. Nilsson, and Y. Yamamoto, "Coherent FSK transmitter using a negative feedback stabilised semiconductor laser," Electron. Lett. **20**, 703–704 (1984).
3. L. Kazovsky, "Performance analysis and laser linewidth requirements for optical PSK heterodyne communications systems," J. Lightwave Technol. **4**, 415–425 (1986).
4. J. M. Kahn, A. H. Gnauck, J. J. Veselka, S. K. Korotky, and B. L. Kasper, "4-Gb/s PSK homodyne transmission system using phase-locked semiconductor lasers," IEEE Photon. Technol. Lett. **2**, 285–287 (1990).
5. F. Herzog, K. Kudielka, D. Erni, and W. Bächtold, "Optical phase locked loop for transparent inter-satellite communications," Opt. Express **13**, 3816–3821 (2005).

#169978 - $15.00 USD Received 6 Jun 2012; revised 4 Sep 2012; accepted 12 Oct 2012; published 22 Oct 2012

6. U. Gliese, T. N. Nielsen, M. Bruun, E. Lintz Christensen, K. E. Stubkjaer, S. Lindgren, and B. Broberg, "A wideband heterodyne optical phase-locked loop for generation of 3–18 GHz microwave carriers," IEEE Photon. Technol. Lett. **4**, 936–938 (1992).
7. L. A. Johansson and A. J. Seeds, "Millimeter-wave modulated optical signal generation with high spectral purity and wide-locking bandwidth using a fiber-integrated optical injection phase-lock loop," IEEE Photon. Technol. Lett. **12**, 690–692 (2000).
8. S. Takasaka, Y. Ozeki, S. Namiki, and M. Sakano, "External synchronization of 160-GHz optical beat signal by optical phase-locked loop technique," IEEE Photon. Technol. Lett. **18**, 2457–2459 (2006).
9. T. von Lerber, S. Honkanen, A. Tervonen, H. Ludvigsen, and F. Küppers, "Optical clock recovery methods: Review (Invited)," Opt. Fiber Technol. **15**, 363–372 (2009).
10. N. Satyan, W. Liang, and A. Yariv, "Coherence cloning using semiconductor laser optical phase-lock loops," IEEE J. Quantum Electron. **45**, 755–761 (2009).
11. T. Y. Fan, "Laser beam combining for high-power, high-radiance sources," IEEE J. Sel. Top. Quantum Electron. **11**, 567–577 (2005).
12. L. Bartelt-Berger, U. Brauch, A. Giesen, H. Huegel, and H. Opower, "Power-scalable system of phase-locked single-mode diode lasers," Appl. Opt. **38**, 5752–5760 (1999).
13. S. J. Augst, T. Y. Fan, and A. Sanchez, "Coherent beam combining and phase noise measurements of ytterbium fiber amplifiers," Opt. Lett. **29**, 474–476 (2004).
14. C. X. Yu, J. E. Kansky, S. E. J. Shaw, D. V. Murphy, and C. Higgs, "Coherent beam combining of large number of PM fibres in 2-D fibre array," Electron. Lett. **42**, 1024–1025 (2006).
15. S. J. Augst, J. K. Ranka, T. Y. Fan, and A. Sanchez, "Beam combining of ytterbium fiber amplifiers (Invited)," J. Opt. Soc. Am. B **24**, 1707–1715 (2007).
16. N. Satyan, W. Liang, A. Kewitsch, G. Rakuljic, and A. Yariv, "Coherent power combination of semiconductor lasers Using optical phase-lock loops (Invited)," IEEE J. Sel. Top. Quantum Electron. **15**, 240–247 (2009).
17. W. Liang, N. Satyan, A. Yariv, A. Kewitsch, G. Rakuljic, F. Aflatouni, H. Hashemi, and J. Ungar, "Coherent power combination of two Master-oscillator-power-amplifier (MOPA) semiconductor lasers using optical phase lock loops," Opt. Express **15**, 3201–3205 (2007).
18. S. A. Diddams, D. J. Jones, J. Ye, S. T. Cundiff, J. L. Hall, J. K. Ranka, R. S. Windeler, R. Holzwarth, T. Udem, and T. W. Hänsch, "Direct link between microwave and optical frequencies with a 300 THz femtosecond laser comb," Phys. Rev. Lett. **84**, 5102–5105 (2000).
19. L.-S. Ma, Z. Bi, A. Bartels, L. Robertsson, M. Zucco, R. S. Windeler, G. Wilpers, C. Oates, L. Hollberg, and S. A. Diddams, "Optical frequency synthesis and comparison with uncertainty at the 10^{-19} Level," Science **303**, 1843–1845 (2004).
20. E. Seise, A. Klenke, S. Breitkopf, M. Plötner, J. Limpert, and A. Tünnermann, "Coherently combined fiber laser system delivering 120μJ femtosecond pulses," Opt. Lett. **36**, 439–441 (2011).
21. S. B. Weiss, M. E. Weber, and G. D. Goodno, "Group delay locking of broadband phased lasers," in "Lasers, Sources, and Related Photonic Devices," (Optical Society of America, 2012), p. AM3A.5.
22. K. Shiraki, M. Ohashi, and M. Tateda, "SBS threshold of a fiber with a Brillouin frequency shift distribution," J. Lightwave Technol. **14**, 50 –57 (1996).
23. J. Hansryd, F. Dross, M. Westlund, P. A. Andrekson, and S. N. Knudsen, "Increase of the SBS threshold in a short highly nonlinear fiber by applying a temperature distribution," J. Lightwave Technol. **19**, 1691–1697 (2001).
24. J. M. C. Boggio, J. D. Marconi, and H. L. Fragnito, "Experimental and numerical investigation of the SBS-threshold increase in an optical fiber by applying strain distributions," J. Lightwave Technol. **23**, 3808–3814 (2005).
25. Y. Aoki, K. Tajima, and I. Mito, "Input power limits of single-mode optical fibers due to stimulated Brillouin scattering in optical communication systems," J. Lightwave Technol. **6**, 710 –719 (1988).
26. G. D. Goodno, S. J. McNaught, J. E. Rothenberg, T. S. McComb, P. A. Thielen, M. G. Wickham, and M. E. Weber, "Active phase and polarization locking of a 1.4 kW fiber amplifier," Opt. Lett. **35**, 1542–1544 (2010).
27. J. O. White, A. Vasilyev, J. P. Cahill, N. Satyan, O. Okusaga, G. Rakuljic, C. E. Mungan, and A. Yariv, "Suppression of stimulated Brillouin scattering in optical fibers using a linearly chirped diode laser," Opt. Express **20**, 15872–15881 (2012).
28. N. Satyan, A. Vasilyev, G. Rakuljic, J. O. White, and A. Yariv, "Phase-locking and coherent power combining of linearly chirped optical waves," in "CLEO:2012 - Laser Science to Photonic Applications," (Optical Society of America, 2012), p. CF2N.1.
29. C. E. Mungan, S. D. Rogers, N. Satyan, and J. O. White, "Time-dependent modeling of Brillouin scattering in optical fibers excited by a chirped diode laser," IEEE J. Quantum Electron. (to be published).
30. N. Satyan, A. Vasilyev, G. Rakuljic, V. Leyva, and A. Yariv, "Precise control of broadband frequency chirps using optoelectronic feedback," Opt. Express **17**, 15991–15999 (2009).
31. F. M. Gardner, *Phaselock Techniques* (Hoboken, NJ: John Wiley and Sons, 2005).
32. L. N. Langley, M. D. Elkin, C. Edge, M. J. Wale, U. Gliese, X. Huang, and A. J. Seeds, "Packaged semiconductor laser optical phase-locked loop (OPLL) for photonic generation, processing and transmission of microwave signals," IEEE Trans. Microw. Theory Tech. **47**, 1257–1264 (1999).

#169978 - $15.00 USD Received 6 Jun 2012; revised 4 Sep 2012; accepted 12 Oct 2012; published 22 Oct 2012

33. C. D. Nabors, "Effects of phase errors on coherent emitter arrays," Appl. Opt. **33**, 2284–2289 (1994).

1. Introduction

Optical phase-locking and phase-synchronization have found applications in a wide variety of fields, including optical communication links [1–5], clock generation and transmission [6, 7], synchronization and recovery [8,9], coherence cloning [10], coherent power combining and optical phased arrays [11–17], and optical frequency standards [18, 19]. These applications take advantage of the ability to precisely synchronize the phase of two optical waves using electronic feedback. With a few notable exceptions [20, 21], prior demonstrations of phase-locking and synchronization have been performed using nominally monochromatic optical waves. In this work, we explore the "dynamic" phase-locking of optical waves whose frequencies are swept ("chirped") rapidly with time and over large chirp extents. Whereas phase-locking optical waves with arbitrary frequency chirps is a difficult problem in general, we show that it is possible to phase-lock linear frequency chirps with a very high locking efficiency. This result is particularly relevant in the context of coherent combining of high-power fiber amplifiers, and also has potential applications in electronic beam steering for LIDAR and 3-D imaging systems.

The output power of optical fiber amplifiers is usually limited by stimulated Brillouin scattering (SBS) in the fiber. The effects of SBS can be mitigated by careful design of the fiber geometry and doping [22–24], and two separate approaches are typically used to obtain even higher output powers: (i) increasing the threshold power for SBS by increasing the linewidth of the seed laser by phase or frequency modulation [25, 26], and (ii) combining the outputs of multiple fiber amplifiers [11–16]. In this work, we investigate a combination of these two approaches in order to enable the combining of fiber amplifiers that have a larger SBS threshold. In particular, we will consider a coherent beam combining approach with active feedback, in a master-oscillator-power-amplifier (MOPA) scheme where multiple fiber amplifiers are seeded by a common seed laser source.

The traditional approach to SBS suppression by broadening the linewidth of the seed laser source results in a reduction of the coherence length of the source, and coherent beam combining therefore requires precise path-length matching so as to prevent dephasing due to incoherence. In recent work, Goodno et. al [26] have demonstrated the phase-locking of a 1.4 kW fiber amplifier using a seed source with a linewidth of 21 GHz, but this required precise path-length matching of active fibers to the order of $\sim$1 mm in order to achieve efficient power combining. Seed lasers with linewidths larger than 100 GHz are necessary to obtain even higher powers, and precise path length matching to within ~ 10 μm is required for coherent combining of multiple amplifiers. Weiss et. al [21] have recently demonstrated that coherent combining can still be achieved using a novel feedback loop that senses the path length mismatch and corrects it using a fiber stretcher.

Our approach is to instead use a rapidly chirped ($> 10^{14}$ Hz/s) laser as the seed source, which increases the SBS threshold in the fiber by reducing the effective length over which SBS occurs in the fiber [27]. The advantage of this approach is that the chirped source is based on a narrow linewidth laser, and therefore has a large coherence length (several meters), which obviates the need for any precise path length matching. In this paper, we describe the phase-locking and electronic phase control of linearly chirped waves using acoustooptic frequency shifters to compensate for static and dynamic optical path-length mismatch and phase noise. We analyze these optical phase-locked loops in the homodyne and heterodyne locking configurations, and present results of proof-of-concept experimental demonstrations of phase-locking, coherent combining, and electronic phase control of passive fiber systems.

The basic concept of phase-locking multiple linearly chirped waves in the MOPA configura-

#169978 - $15.00 USD Received 6 Jun 2012; revised 4 Sep 2012; accepted 12 Oct 2012; published 22 Oct 2012

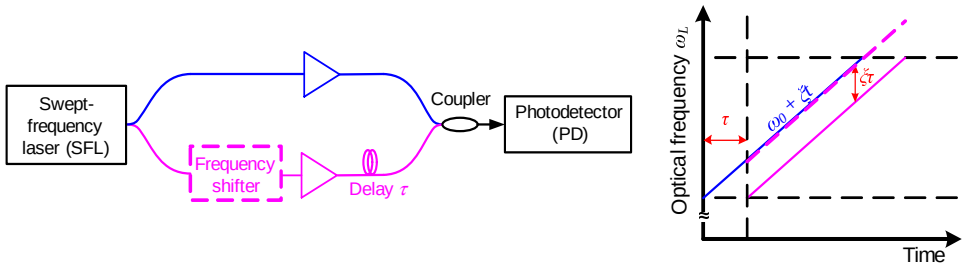

Fig. 1. Concept of phase-synchronization of linearly chirped waves. A time delay between the master and slave arms is equivalent to a frequency delay, and can be compensated using an optical frequency shifter.

tion is depicted in Fig. 1 [28]. A common swept-frequency laser (SFL) with a perfectly linear optical frequency chirp given by

$$\omega_L(t) = \omega_0 + \xi t,\ t \in [0, T], \tag{1}$$

is split into multiple arms that are separately amplified, and coherently combined to form a high-power beam. Consider two arms with a relative time delay τ. Owing to the linearity of the chirp, the time delay is equivalent to a frequency difference $\delta\omega = \xi\tau$ between the two waves, and an optical frequency shifter—such as an acoustooptic shifter—in one of the arms can provide the desired frequency shift to synchronize the phases of the two waves. For a linear chirp of $\xi/2\pi = 10^{15}$ Hz/s and a path-length mismatch of 10 cm in fiber, the required frequency shift is 500 kHz, which is well within the dynamic range of acoustooptic frequency shifters. Further, using a negative feedback phase-locked loop architecture with the frequency shifter operating as a voltage-controlled oscillator, dynamic phase fluctuations are also suppressed for frequencies within the loop bandwidth. Previous work using acoustooptic frequency shifters and monochromatic seed lasers has shown that sufficient loop bandwidths can be achieved for efficient combining of active fiber amplifiers [13].

In this paper, we consider the phase-locking and coherent combining of optical waveforms whose frequencies vary perfectly linearly with time, as shown in Fig. 2. The motivation for the choice of triangular frequency modulation is twofold. First, SBS suppression in high power amplifiers scales with the chirp rate [27, 29], and a constant chirp rate ensures that uniform SBS suppression is obtained throughout the duration of the frequency sweep, with minimal increase of the SBS at the turning points of the chirp. Second, a linear chirp enables path-length mismatches to be corrected by a constant frequency shift, as described above. Deviations from linearity of the seed laser chirp are corrected using a feedback loop, as long as these deviations are small and at frequencies within the loop bandwidth. It is desirable that the chirp be close to perfectly linear, particularly at high chirp rates ξ, in order to relax the requirements on the frequency tuning range and bandwidth of the acoustooptic frequency shifter and the feedback loop. We note that it is possible to further extend this approach to other deterministic frequency chirp formats, by using a time-varying frequency shift to compensate for the known time-varying slope of the optical frequency chirp, e.g. using a feedforward compensation scheme.

2. Precisely linear frequency chirps using an optoelectronic swept-frequency laser

A perfectly linear optical frequency-vs-time behavior is a prerequisite for the phase-locking scheme shown in Fig. 1. We have previously shown that such a precisely linear chirp can be generated using a semiconductor laser in a negative feedback loop [30]. The tuning of the

#169978 - $15.00 USD Received 6 Jun 2012; revised 4 Sep 2012; accepted 12 Oct 2012; published 22 Oct 2012

frequency of the semiconductor laser via its injection current eliminates any moving parts, and the optoelectronic SFL is capable of generating high-speed linear frequency chirps over wide tuning ranges. The operation of the SFL is briefly summarized below, and a more detailed analysis is presented in Ref. [30].

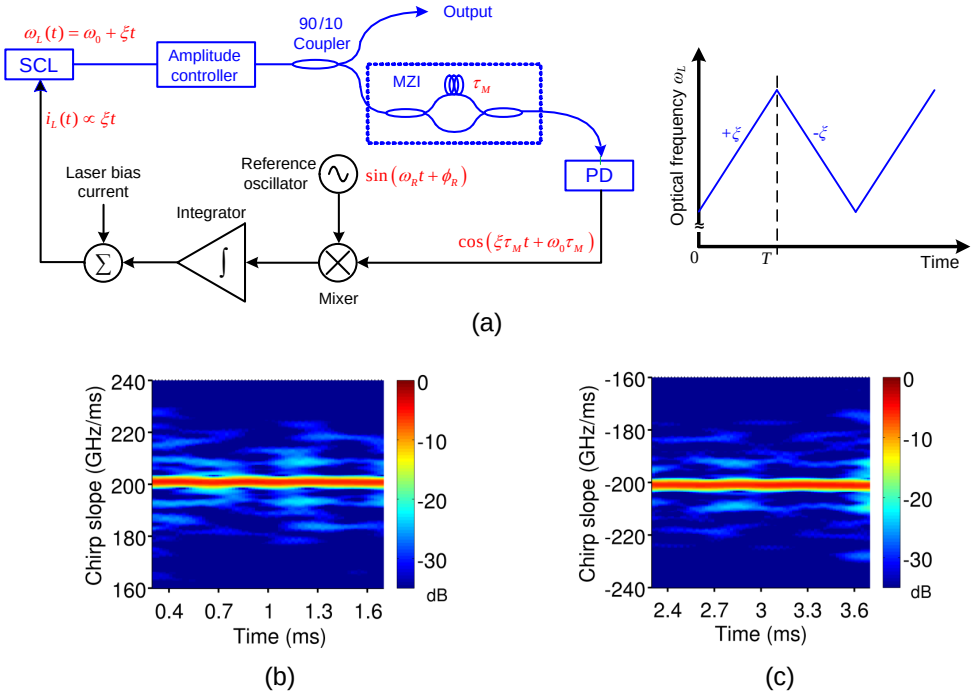

Fig. 2. (a) Schematic diagram of an optoelectronic SFL using a semiconductor laser in a negative feedback loop. SCL: Semiconductor laser, MZI: Mach-Zehnder interferometer, PD: Photodetector. (b) and (c) Measured slope of the optical frequency chirp during the up- and down-chirps respectively, for an optoelectronic SFL using a vertical cavity surface emitting laser. The chirp rate is $\pm 2 \times 10^{14}$ Hz/s, corresponding to a frequency excursion of $\pm$400 GHz in 2 ms.

A schematic diagram of the optoelectronic feedback loop is shown in Fig. 2(a). The frequency vs. current behavior of the semiconductor laser is highly nonlinear owing to its thermal tuning mechanism. The laser is biased with a time-varying injection current, and its frequency chirp is linearized using a negative feedback loop—a phase-locked loop—whose operation may be understood intuitively as follows. The slope of the laser frequency chirp is proportional to the input current into the loop integrator, assuming the laser is a linear tuning element. This assumption is valid for small signal fluctuations about the laser bias current. When a linear frequency chirp $\omega_L(t)$ of the form in Eq. (1) is passed through a Mach-Zehnder interferometer (MZI) with delay τ_M and is incident on a photodetector (PD), the resultant current has the form $\cos(\xi \tau_M t + \omega_0 \tau_M)$. The combination of the integrator, laser, MZI and PD therefore acts as an effective current-controlled oscillator, where the output frequency deviation of the photocurrent is proportional to the input current into the integrator. This "oscillator" is phase-locked to an electronic oscillator whose output is of the form $\sin(\omega_R t + \phi_R)$. In lock, the chirp parameters

#169978 - $15.00 USD Received 6 Jun 2012; revised 4 Sep 2012; accepted 12 Oct 2012; published 22 Oct 2012

are therefore given by

$$\begin{aligned} \xi &= \frac{\omega_R}{\tau_M}, \\ \omega_0 &= \frac{\phi_R + 2m\pi}{\tau_M}, \end{aligned} \tag{2}$$

where m is an integer. The slope of the optical frequency chirp is therefore set by the frequency of the electronic oscillator. A triangular frequency deviation, as shown in Fig. 2(a), is obtained by appropriately driving the laser bias current.

The experimental demonstrations in this work were performed using an optoelectronic SFL based on a vertical cavity surface-emitting laser (VCSEL) at 1550 nm in the optoelectronic feedback loop shown in Fig. 2(a). An amplitude controller based on a semiconductor optical amplifier was used to maintain a constant output power level. While the SFL is capable of producing precisely linear chirps with chirp rates up to 10^{16} Hz/s, a chirp-rate of $\pm 2 \times 10^{14}$ Hz/s—corresponding to a frequency excursion of $\pm$400 GHz in 2 ms—was used in the experimental demonstrations in this work. As described in the previous paragraph, the instantaneous optical chirp rate of the SFL can be measured using an MZI and a photodetector. The measured values of the optical chirp rate for the up- and down-chirps, using an MZI with a time-delay of 1.03 ns, are plotted in Figs. 2(b) and 2(c), demonstrating the linearity of the chirp.

3. Phase-locking of chirped optical waves

3.1. Homodyne phase-locking

3.1.1. Theory

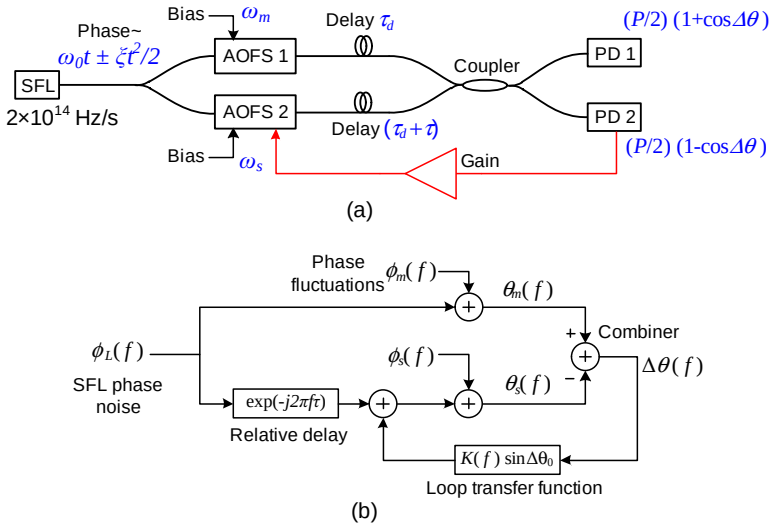

Fig. 3. (a) Fiber-based homodyne phase-locking configuration. The upper and lower arms are the master and slave waveforms respectively. SFL: swept-frequency laser, PD: photodetector. (b) Small signal model of phase propagation in the loop. The variables are the Fourier transforms of the deviations of the phases from their steady-state values.

We first consider the homodyne phase-locking configuration shown in Fig. 3(a). The output of an optoelectronic SFL is split into two arms using a fiber splitter, and combined using a 2×2

#169978 - $15.00 USD Received 6 Jun 2012; revised 4 Sep 2012; accepted 12 Oct 2012; published 22 Oct 2012

fiber combiner. The goal of the experiment is to phase-lock the output of the "slave" arm to the "master" arm. Acoustooptic frequency shifters with bias frequency shifts ω_m and ω_s are used in the master and slave arms respectively. The differential delay between the two arms is given by τ. One of the fiber combiner output channels serves as the useful optical output, while the other channel is amplified and fed back to the acoustooptic frequency shifter in the slave arm. The feedback loop is very similar to a typical phase-locked loop [31], and can be analyzed accordingly. The loop gain K is defined as the product of the optical power in each arm ($P/2$, units: W), the gain of the photodetector (V/W), and the gains of the loop amplifier (V/V) and the frequency shifter (rad/s/V). Let the SFL optical frequency be given by Eq. (1). The phase difference between the master and slave arms is denoted by $\Delta\theta \equiv \theta_m - \theta_s$, and is given by

$$\begin{aligned}\Delta\theta(t) &= \left[(\omega_0+\omega_m)t+\frac{1}{2}\xi t^2+\phi_m\right] \\ &\quad -\left[(\omega_0+\omega_s)(t-\tau)+\frac{1}{2}\xi(t-\tau)^2+\int_0^{t-\tau_d}K\left(1-\cos\Delta\theta(t')\right)\mathrm{d}t'\right], \end{aligned} \quad (3)$$

where ϕ_m is a constant phase difference between the two arms, and we assume that the loop propagation delay τ_d is much larger than the path-length mismatch τ. The final term in Eq. (3) represents the phase shift due to the feedback to the acoustooptic frequency shifter, which is the integral of the frequency shift. The steady-state solution to Eq. (3) is obtained by setting the time derivative of $\Delta\theta$ to 0, to obtain

$$\Delta\theta_0 = \cos^{-1}\left[1-\frac{(\omega_m-\omega_s+\xi\tau)}{K}\right] \equiv \cos^{-1}\left(1-\frac{\Delta\omega_{\mathrm{fr}}}{K}\right). \quad (4)$$

The quantity $\Delta\omega_{\mathrm{fr}} \equiv \omega_m - \omega_s + \xi\tau$ is the *free-running* frequency difference between the master and slave arms, and the phase-locked loop adjusts the value of $\Delta\theta_0$ to bring the loop into lock. When in lock the two optical waves only differ by a phase $\Delta\theta_0$ at the combiner, and there is no frequency difference. We note here that the value of the steady-state phase can be adjusted (within the range $[0,\pi]$) by varying the bias frequency shifts ω_m and ω_s.

The loop can be linearized about the steady-state operating point of Eqs. (3) and (4) in order to understand its dynamic performance. The Fourier transform of the small signal deviations from the steady-state solution are used in this analysis, as shown in Fig. 3(b). For simplicity, we have not included the effects of amplitude noise and shot noise in the photodetector, but these can be incorporated into the analysis in a straightforward manner. The phase noise added to the master and slave arms are denoted by $\phi_m(f)$ and $\phi_s(f)$ respectively, and include the phase noise of the frequency shifters and the noise $\omega_0\delta\tau(f)$ due to fluctuations ($\delta\tau$) of the optical path length. The phase noise (including residual chirp non-linearity) of the SFL is given by $\phi_L(f)$, and is delayed by an additional amount τ in the slave arm. The frequency dependence of the loop gain is modeled by $K(f)$, which is given by

$$K(f) = \frac{K_{\mathrm{el}}(f)\exp(-j2\pi f\tau_d)}{j2\pi f}. \quad (5)$$

The pole $1/(j2\pi f)$ is the consequence of the frequency shifter behaving as an integrator with respect to the phase, $K_{\mathrm{el}}(f)$ is the frequency response of the loop electronics, and the exponential term is the effect of the loop propagation delay τ_d. The solution to the feedback loop is then given by

$$\begin{aligned}\Delta\theta(f) &= \frac{\phi_m(f)-\phi_s(f)}{1+K(f)\sin\Delta\theta_0}+\frac{\phi_L(f)\left(1-e^{-j2\pi f\tau}\right)}{1+K(f)\sin\Delta\theta_0} \\ &\cong \frac{\phi_m(f)-\phi_s(f)}{1+K(f)\sin\Delta\theta_0}+\frac{\tau[j2\pi f\phi_L(f)]}{1+K(f)\sin\Delta\theta_0}. \end{aligned} \quad (6)$$

#169978 - $15.00 USD Received 6 Jun 2012; revised 4 Sep 2012; accepted 12 Oct 2012; published 22 Oct 2012

The first term in the above expression demonstrates the reduction of the phase fluctuations in the fiber by a factor $(1+K(f)\sin\Delta\theta_0)$. For frequencies within the loop bandwidth, $K(f)$ is a large number, and efficient noise suppression is obtained. The second term describes the effect of SFL phase noise. For small delays τ, the system behaves like a frequency discriminator with gain τ, and this frequency noise is also suppressed by the factor $(1+K(f)\sin\Delta\theta_0)$. It is clear that a smaller delay and an SFL with low phase noise result in lower phase error in the loop.

3.1.2. Experiment

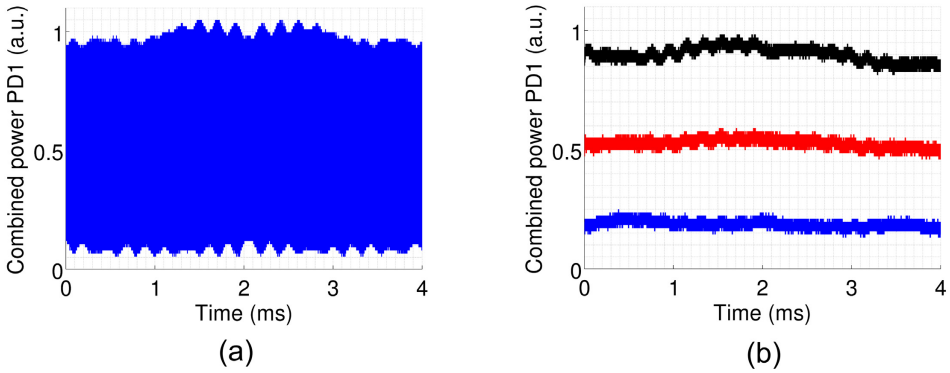

Fig. 4. Experimental results of homodyne phase-locking of two chirped optical waves. (a) Unlocked combining, where the path-length mismatch results in a rapid oscillation of the combined power. (b) Phase-locked operation, for different values of the free-running frequency difference $\Delta\omega_{\rm fr}$. The SFL chirps +400 GHz in the first 2 ms, and −400 GHz in the next 2 ms.

The homodyne phase-locking experiment of Fig. 3(a) was performed using the VCSEL optoelectronic SFL with a chirp rate of 2×10^{14} Hz/s shown in Fig. 2. Polarization-maintaining fiber-optic components were used in the loop. A passive delay of $\tau_d\approx20$ m in fiber was introduced in each arm, in order to study the loop performance in the presence of large delays such as those introduced by fiber amplifiers. The nominal path length difference between the two arms was $\tau\approx0$, but no special care was taken to ensure path-length matching, and we estimate an accuracy of ±2 cm. Fiber-coupled acoustooptic modulators (Brimrose Corporation) with a nominal frequency shift of 100 MHz and a frequency modulation bandwidth of ~75 kHz were used in each arm. An op-amp based electronic amplifier was used in the loop to provide the necessary gain. Amplified photodetectors (Thorlabs) with a bandwidth of 150 MHz were used to measure the combined signals. The measured output at the photodetector PD1 is plotted in Fig. 4(a) and 4(b) for the unlocked and phase-locked cases respectively. The free-running frequency difference $\Delta\omega_{\rm fr}$ was adjusted, via the bias of one AOFS, to bring the loop into lock, and to vary the fraction of power in the useful arm, as given by Eq.(4). Note that the sign of the optical chirp ξ reverses at $t=2$ ms, and the bias frequency shift was therefore periodically adjusted using a custom arbitrary waveform generator to maintain the same locked phase along both the up- and down-chirps.

The homodyne phase-locking approach demonstrated above has a few shortcomings. 1) Intensity fluctuations at the photodetector due to variations in the laser power—as seen in the non-constant envelope of the oscillations in Fig. 4(a)—cannot be decoupled from the phase fluctuations to be corrected by the loop, and the phase-locked output (Fig. 4(b)) is affected by these fluctuations. This problem can be mitigated using a balanced detection scheme, but the

#169978 - $15.00 USD Received 6 Jun 2012; revised 4 Sep 2012; accepted 12 Oct 2012; published 22 Oct 2012

loop is still susceptible to large $1/f$ photodetector noise at low frequencies. 2) The desired operating point for maximum power-combining is $\Delta\theta_0 \approx 0$ in Eq. (4); however, from Eq. (6), the loop gain is multiplied by $(\sin\Delta\theta_0)$, and the loop is consequently not very stable at this operating point. It is desirable that the loop be locked at quadrature ($\Delta\theta_0 = \pi/2$), and the control of the optical phase by varying the free-running frequency difference is not optimal since it adversely impacts loop performance. 3) Finally, it is not straightforward to scale this approach to multiple phase-locked arms. These problems are all addressed by adopting a heterodyne (or offset) phase-locking architecture, as described in the next section.

3.2. Heterodyne (offset) phase-locking

3.2.1. Theory

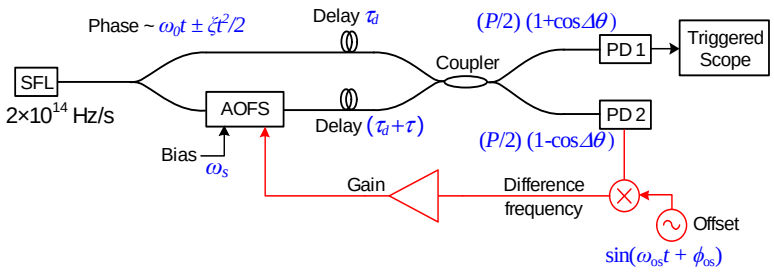

Fig. 5. Fiber-based heterodyne phase-locking configuration. The offset frequency of the loop is 100 MHz. SFL: swept-frequency laser, PD: photodetector.

The heterodyne phase-locking architecture is shown in Fig. 5, where the chirped slave path is locked to the master arm at a frequency offset determined by an electronic oscillator. The two optical waves are mixed in a photodetector, resulting in an oscillating photocurrent at the difference frequency between the two waves. This photocurrent is mixed with an electronic oscillator $\sin(\omega_{os}t + \phi_{os})$ using an electronic mixer. The difference frequency output of the mixer is amplified, and fed back into the AOFS. This loop can be analyzed in the same way as the homodyne loop of Section 3.1, using standard phase-locked loop theory [31]. Defining the loop gain as the product of the SFL power in each arm and the gains of the photodetector, mixer, loop amplifier and the AOFS; and setting the time-derivative of the mixer output to zero, we obtain the steady state phase difference between the master and slave arms ($\Delta\theta \equiv \theta_m - \theta_s$):

$$\Delta\theta_0 = -\omega_{os}t - \phi_{os} - \sin^{-1}\left(\frac{\omega_s - \xi\tau - \omega_{os}}{K}\right) \equiv -\omega_{os}t - \phi_{os} - \sin^{-1}\left(\frac{\Delta\omega_{fr}}{K}\right). \qquad (7)$$

The phase of the slave optical wave now follows that of the master wave with a frequency and phase offset determined by the offset electronic oscillator. A number of slave arms may be locked to a common master wavefront with the same electronic offset frequency ω_{os}, for coherent power combining. The advantage of heterodyne locking is that it enables electronic control over the phase of the chirped slave optical wave, since a change in ϕ_{os} is reflected in a change in the optical phase in a one-to-one manner. This electronic phase control is important for beam-steering and phase-controlled optical apertures. The final term in Eq. (7) is the loop phase error $\theta_{loop} \equiv \sin^{-1}(\Delta\omega_{fr}/K)$, which may be brought close to zero by adjusting the bias frequency shift of the AOFS. A small-signal phase noise analysis may be performed about the steady-state operating point, using a model very similar to Fig. 3(b), except for the addition of

#169978 - $15.00 USD Received 6 Jun 2012; revised 4 Sep 2012; accepted 12 Oct 2012; published 22 Oct 2012

the phase noise $\phi_{os}(f)$ of the electronic offset oscillator. The resultant output phase error is

$$\Delta\theta(f) = \frac{\phi_m(f) - \phi_s(f)}{1 + K(f)\cos\theta_{loop}} + \frac{\tau\,[j2\pi f\phi_L(f)]}{1 + K(f)\cos\theta_{loop}} - \frac{\phi_{os}(f)K(f)\cos\theta_{loop}}{1 + K(f)\cos\theta_{loop}}. \quad (8)$$

The first two terms are identical in form to Eq. (6), while the final term shows that the phase noise of the electronic offset source is transferred to the optical wave, and should be kept as small as possible.

3.2.2. Experiment

The heterodyne phase-locking experiment of Fig. 5 was performed using the VCSEL-based SFL with a chirp rate of $\pm 2 \times 10^{14}$ Hz/s, polarization maintaining fiber-optic components, and an AOFS (Brimrose Corporation) with a frequency shift of 100 MHz and a frequency modulation bandwidth of ~ 75 kHz. The two arms were mixed in an amplified photodetector (Thorlabs) with a bandwidth of 150 MHz, and the resultant beat signal was mixed with an electronic offset signal in a discrete electronic mixer (MiniCircuits). The mixer output was amplified and fed back into the AOFS. The 100 MHz electronic offset signal was derived from a custom-built direct digital synthesis (DDS) oscillator with adjustable amplitude, phase and frequency. A custom arbitrary waveform generator was used to provide the different AOFS bias frequencies during the up- and down-chirps, in order to maintain the same free-running frequency difference. The experiment was performed for different values of the loop propagation delay τ_d and path-length mismatch τ. The optical delay is reported here in units of length, and is to be understood as the time taken for light to propagate along that length of polarization-maintaining Panda fiber.

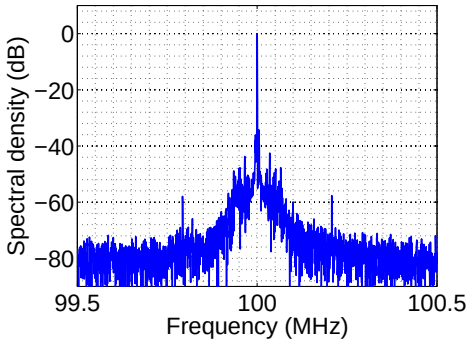

Fig. 6. Fourier spectrum of the measured beat signal between the master and phase-locked slave arms, over a 2 ms chirp interval. The nominal loop delay parameters are $\tau_d = 20$ m and $\tau = 0$ m of fiber. A Hamming window was used in the calculation to eliminate the spectral sidebands due to the finite measurement time.

The performance of the heterodyne phase-locked loop was characterized by measuring the beat signal between the master and slave arms using the photodetector PD1 and a high-speed (1.6 ns) sampling oscilloscope. In lock, the oscillating component of the photocurrent has the form

$$i(t) \propto \cos\left(\Delta\theta_0 + \Delta\theta(t)\right) = \cos\left(\omega_{os}t + \phi_{os} + \theta_{loop} - \Delta\theta(t)\right), \quad (9)$$

where the phase fluctuations $\Delta\theta(t)$ are described in the frequency domain by Eq. (8). The variance of these phase fluctuations, $\langle\Delta\theta^2\rangle$, is the critical metric of loop performance since it determines the fraction of the slave power that is coherent with the master laser [16, 32]. The

#169978 - $15.00 USD Received 6 Jun 2012; revised 4 Sep 2012; accepted 12 Oct 2012; published 22 Oct 2012

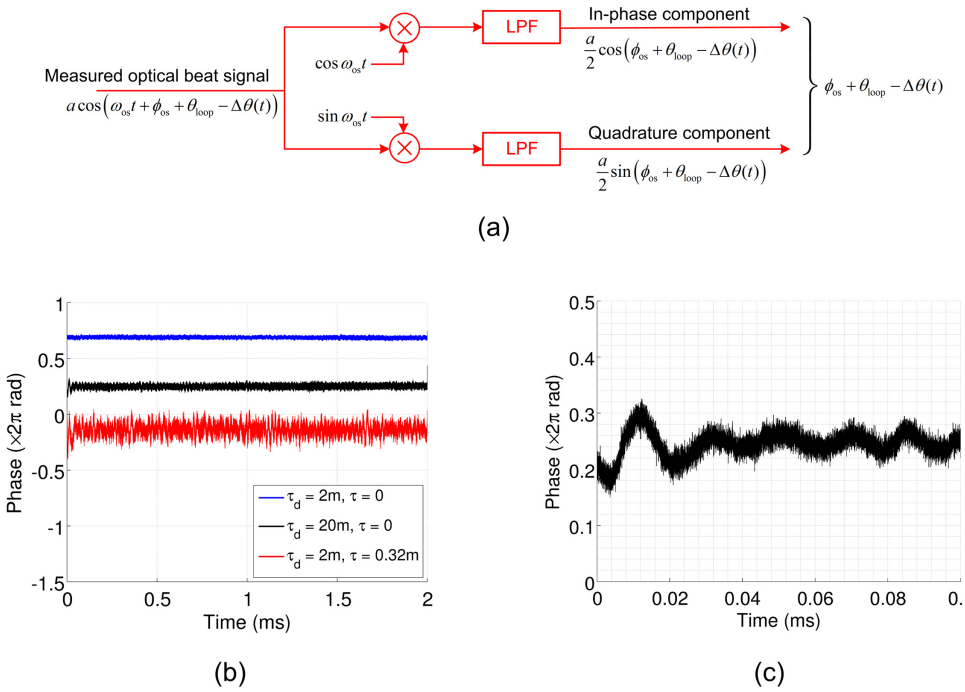

Fig. 7. (a) Algorithm for calculation of the relative phase between the master and phase-locked slave beams from the measurement of the beat signal between the two waves. LPF: Low-pass filter. (b) Phase difference between the master and slave arms for different values of the loop delay τ_d and the path-length mismatch τ. (c) Transient during the switching of the chirp from an SFL down-chirp to up-chirp. The bandwidth (locking time) is limited by the AOFS driver used in the experiment.

Fourier transform of the measured beat signal over one 2 ms chirp duration (with a Hamming window to eliminate edge effects), for $\tau_d = 20$ m and $\tau \approx 0$, is plotted in Fig. 6, showing a transform-limited peak at 100 MHz, with a small noise pedestal. The loop bandwidth is about 60 kHz, limited by the electronic driver for the AOFS, and can be improved using a faster RF driver. The residual noise may be calculated by integrating the noise in the spectral measurement [16, 32]. From Fig. 6, the standard deviation of the phase fluctuations is calculated to be 0.08 rad, which corresponds to 99.4% of the slave optical power being coherent with the master wave.

We further characterize the phase fluctuations using a phase demodulation technique, which allows us to directly calculate and characterize the phase fluctuations $\Delta\theta(t)$ as a function of time. The phase demodulation algorithm is shown in Fig. 7(a). The components of the measured beat signal $\cos\left(\omega_{os}t+\phi_{os}+\theta_{loop}-\Delta\theta(t)\right)$ along the two quadrature axes $\cos\omega_{os}t$ and $\sin\omega_{os}t$ (also called In-phase and Quadrature or I/Q components) are calculated, from which the phase $\phi_{os}+\theta_{loop}-\Delta\theta(t)$ is computed. Since the first two terms are constant, this allows us to directly characterize the fluctuations of the phase with time. The demodulated phase during one 2 ms chirp duration for three different values of the loop delay τ_d and the path-length mismatch τ are plotted in Fig. 7(b). The curves are offset by different phases, for the sake of clarity. The initial transient owing to the limited loop bandwidth is shown in Fig. 7(c).

The standard deviation of the phase error can directly be calculated from the demodulated phase, ignoring the initial transient, and the achieved phase error for different delays are tabu-

#169978 - $15.00 USD Received 6 Jun 2012; revised 4 Sep 2012; accepted 12 Oct 2012; published 22 Oct 2012

lated in Table 1. Note that the fiber delays are only nominal values, since no extra effort was made to precisely cut fibers. We estimate the accuracy of the fiber length to be ± 2 cm. For a given path-length mismatch, the addition of a large loop delay $\tau_d = 20$ m slightly reduces the bandwidth of the loop, resulting in a lower phase-locking efficiency. On the other hand, for a given loop delay, the addition of 32 cm of path-length mismatch results in increased phase-noise due to a loss of coherence, as given by Eq. (8). This reduces the phase-locking efficiency from $\sim 99\%$ to $\sim 90\%$, as shown in Table 1. Path-length mismatches much smaller than 32 cm are very easily achieved in practice, corresponding to phase-locking efficiencies larger than 90%.

Table 1. Measured residual phase error and phase-locking efficiency for different values of the loop delay τ_d and the path-length mismatch τ.

Loop delay τ_d (m)	Path-length mismatch τ (cm)	Phase error $\sigma = \langle \Delta\theta^2(t) \rangle^{1/2}$ (rad)	Locking efficiency $\eta = 1/(1+\sigma^2)$
2	0	0.047	99.8%
2	32	0.279	92.8%
20	0	0.076	99.4%
20	32	0.315	91.0%

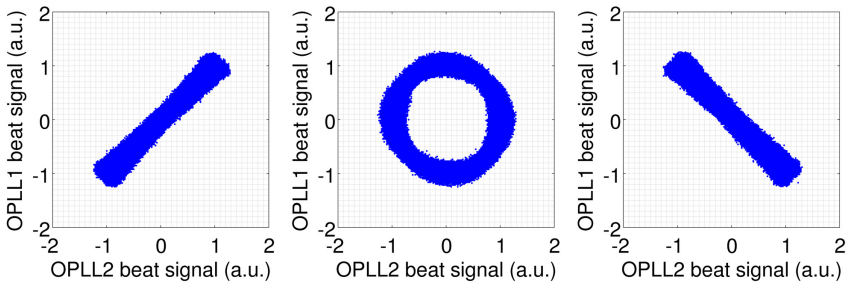

Fig. 8. Measured optical beat signals between the slave and master chirped waves in two distinct phase-locked loops, with synchronized offset electronic signals with a frequency $\omega_{os} = 100$ MHz. The phase ϕ_{os} of one of the electronic oscillators was set to 0°, 90° and 180° in the three panels, which is reflected in a change in the optical phase of the slave laser phase by the same amount. The delays in each loop were $\tau_d = 2$ m and $\tau \approx 0$.

To demonstrate electronic control over the phase of the chirped optical wave, we constructed two separate heterodyne optical phase-locked loops derived from the same SFL. The SFL output was split into four paths using fiber splitters. Two of these paths acted as master wavefronts for two distinct slave arms, and the two loops were locked at the same offset frequency ω_{os} in fiber-based loops. The electronic offset signals were provided by a pair of synchronized DDS oscillators, with individually controllable amplitudes and phases. The beat signals in the two OPLLs were measured over a 2 ms chirp duration, and are plotted against each other in Fig. 8. As the electronic phase ϕ_{os} in one of the arms was changed, the phase of the optical beat signal changed in a one-to-one manner, demonstrating digital phase-control.

4. Coherent combining and phase-controlled apertures

The phase-locking of slave arms to a master wavefront can be scaled to multiple fiber paths, as shown in the tiled-aperture coherent combining experiment in Fig. 9(a). A small portion of the output of each amplified slave arm is beat with a common master wavefront, and phase-locked

#169978 - $15.00 USD Received 6 Jun 2012; revised 4 Sep 2012; accepted 12 Oct 2012; published 22 Oct 2012

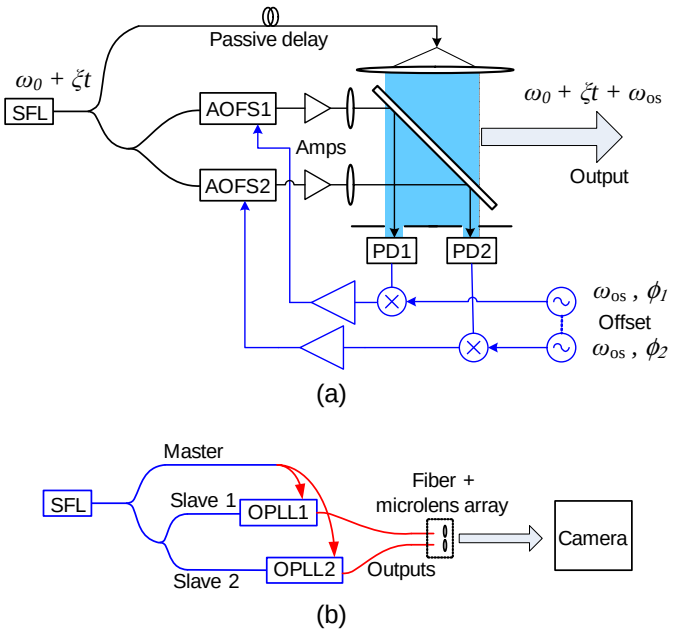

Fig. 9. (a) Schematic diagram of a tiled-aperture coherent combining experiment with multiple chirped amplifiers. (b) Schematic diagram of a proof-of-concept passive fiber-based experiment to demonstrate electronic beam steering. The fiber path-length mismatches not corrected by the optical phase-locked loops are shown in red. The camera is placed in the far field of the output aperture.

to a set of synchronized electronic oscillators that have the same frequency and individual phase control. The results of such an active-fiber coherent combining experiment will be reported separately; here we describe a proof-of-concept passive fiber-based experiment to demonstrate the principle of electronic control of a chirped optical phased array. A schematic diagram of the fiber-based experiment is shown in Fig. 9(b), which is different from Fig. 9(a) in two ways. First, the master wavefront was split using a fiber splitter and delivered to the two optical phase-locked loops. Second, the output of each slave path (after the AOFS and additional fiber delay) was split into two parts using a fiber splitter: one part was used for phase-locking as in Fig. 5, while the other part formed the useful optical output aperture. This implies that differential delays in these additional fiber paths, shown in red in Fig. 9(b) are not accounted for by the phase-locked loop. In the experimental demonstration, an effective precise path-length matching was achieved by simply phase-locking the two loops at slightly different offset frequencies. As described throughout this paper, the perfect linearity of the chirp means that a frequency shift is equivalent to a time delay. In addition, the fiber portions outside the phase-locked loops were isolated thermally and acoustically to minimize dynamic fluctuations of the path length over the measurement time of the experiment (a few minutes). It is important to note that no path-length matching efforts are necesssary in the free-space experiment of Fig. 9(a).

The outputs of the two phase-locked slave arms were brought together to form a coherent aperture using a fiber V-groove array placed at the focal plane of a microlens array. The emitter spacing was 250 μm. The loop parameters were $\tau_d = 2$ m and $\tau \approx 0$. A camera with a low frame rate was used to image the far-field intensity distribution of the aperture. The frame rate of the camera was more than an order of magnitude smaller than the chirp repetition rate, which ensured that the intensity distribution was measured across many chirp periods. The

#169978 - $15.00 USD Received 6 Jun 2012; revised 4 Sep 2012; accepted 12 Oct 2012; published 22 Oct 2012

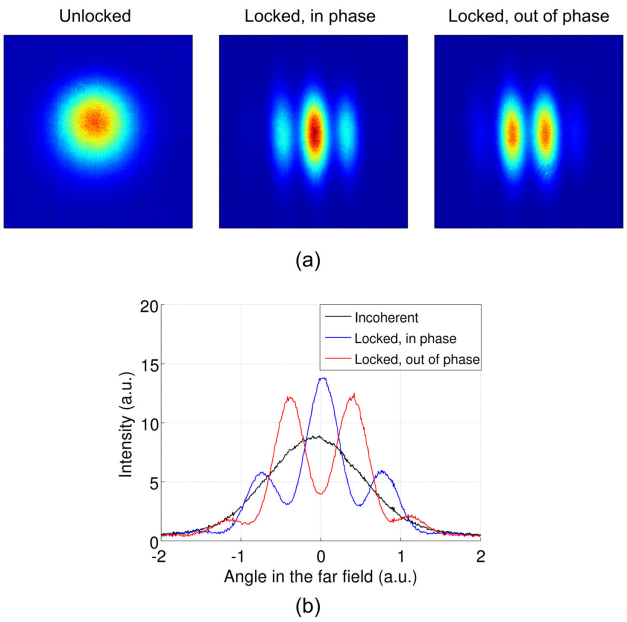

Fig. 10. Experimental demonstration of electronic phase control and beam steering of chirped optical waves. (a) Far-field intensity profiles for the unlocked and phase-locked cases. The position of the fringes is controlled by varying the phase of the electronic oscillator in one loop. (b) Horizontal cross-section of the far-field intensity pattern.

experimentally measured far-field intensity profiles for the unlocked and phase-locked cases are shown in Fig. 10. Compared to incoherent combination, the phase-locked (in-phase) beam has a narrower central lobe whose intensity is larger by a factor of 1.6. By electronically varying the phase of the electronic oscillator in one of the optical phase-locked loops, we demonstrate the steering of the far field intensity pattern, as shown in Fig. 10.

The visibility of the fringes in Fig. 10 is limited by phase fluctuations introduced by the uncompensated fiber segments, shown in red in Fig. 9(b), and wavefront aberrations in the combining optics. In addition, no effort was made to match the polarizations of the two combining beams. When the free-space experiment of Fig. 9(a) is used, the fringe visibility is expected to improve towards a value limited by the residual loop phase error, given by Table 1. The demonstrated coherent combining approach also scales well to larger systems, since the combination of coherent signal gain and incoherent phase errors leads to a higher interferometric visibility with increasing number of optical beams (e.g., see [33]).

5. Summary and discussion

We have analyzed and demonstrated the phase-locking and electronic phase control of optical waves whose frequencies are swept rapidly over large chirp extents. Precisely linear optical frequency chirps generated using an optoelectronically controlled swept-frequency laser (SFL) were used for coherent combining in a master-oscillator-power-amplifier (MOPA) configuration, wherein the linearity of the optical chirp enabled optical delays to be electronically compensated using acoustooptic frequency shifters. In proof-of-principle experiments, we have demonstrated the phase-locking of optical waves that chirp over a frequency range of 400 GHz in 2 ms—i.e., a chirp rate of $\pm 2 \times 10^{14}$ Hz/s—in both the homodyne and heterodyne configurations, and have shown the ability to electronically control the phase and direction of the optical

#169978 - $15.00 USD Received 6 Jun 2012; revised 4 Sep 2012; accepted 12 Oct 2012; published 22 Oct 2012

beam as its frequency is chirped with time. Feedback loop bandwidths of ~ 60 kHz and phase error variances of < 0.01 rad^2 were obtained. The use of an SFL as a seed laser for a high-power optical amplifier has the potential to increase the SBS threshold, leading to larger achievable output power from a single amplifier; and the coherent combining of multiple chirped amplifier outputs can therefore lead to larger powers than using single frequency amplifier arrays. The experimental demonstrations of phase-locking in this work were performed using passive fiber delays in the feedback loops; however, the addition of active fibers with comparable delays results in predominantly low-frequency noise [13,15] which is well within the demonstrated loop bandwidths, and should therefore be corrected by the loop. The experiments were performed at a chirp rate of 2×10^{14} Hz/s, at which rate we have observed significant SBS suppression in long fiber segments [27]. Higher chirp rates may be necessary for efficient SBS suppression in high-power amplifiers with short active fibers, and the demonstration can be scaled to faster chirp rates using optoelectronic SFLs and faster electronic components in the combining system.

Acknowledgments

The authors acknowledge the support of the U.S. Army Research Office (W911NF-11-2-0081) and the High Energy Laser Joint Technology Office (11-SA-0405).

#169978 - $15.00 USD Received 6 Jun 2012; revised 4 Sep 2012; accepted 12 Oct 2012; published 22 Oct 2012